5-1-2024

Mast Cells in Mammary Carcinoma

Alexandria M. Ashbaugh
University of Northern Colorado

University of Northern Colorado
Greeley, CO

Mast Cells in Mammary Carcinoma

A Thesis Submitted in Partial Fulfillment for
Graduation with Honors Distinction and
the Degree of Bachelor of Science
Chemistry

Alexandria M. Ashbaugh

College of Natural and Health Sciences, School of Biological Sciences

May 2024

Mast Cells in Mammary Carcinoma

PREPARED BY_____
Alexandria M. Ashbaugh

APPROVED BY
THESIS ADVISOR: _____
Nicholas A. Pullen, Ph.D.

HONORS
DEPT LIAISON: _____
Stephen P. Mackessy, Ph.D.

HONORS CHAIR: _____
Corinne Wieben

RECEIVED BY THE THESIS PROJECT COMMITTEE ON:

05/04/2024

ABSTRACT

Breast cancer (BC) is an aggressive disease that takes the lives of thousands of women every year. Although knowledge and treatment of this disease have improved over the years, much is still to be discovered about BC. One area of expertise that we are currently trying to learn more information about is the mast cell (MC) and its role in BC growth and development. The MC is an immune system component discovered in tumors' extracellular matrix (ECM). As a tumor grows within body tissues, the tumor recruits the MC from surrounding connective tissues to the tumor, using signaling cytokines such as IL-6 and TGF-β. However, it is understood that depending on the ECM, the MC could exhibit pro or antitumorigenic factors; both have been observed in BC (Aponte-Lopez et al., 2018). This difference in the role of the MC between tumors is attributed to the type of BC; the different activated or over-expressed receptors can cause a different response by the body and the MCs themselves. This study aims to identify unique MC receptors, such as FcεR-I, which could be the target of treatments developed in the future for BC.

ACKNOWLEDGMENTS

The following honors research project was completed with the help of my thesis advisor, Dr. Nicholas A. Pullen, who provided guidance and support in learning the techniques required for this project. Dr. Patrick D. Burns, for his help in confocal microscopy troubleshooting and sample preparation. Viva J. Rasé for her initial sample acquisition. Madison F. Gremillion and Cari A. Alps for their help in data collection. The University of Northern Colorado Office of Undergraduate Research for funding this project.

TABLE OF CONTENTS

LIST OF FIGURES

LIST OF TABLES

INTRODUCTION

Breast cancer (BC) is a complex disease with many moving parts. BC is one of the leading causes of death in women (American Cancer Society, 2021). Even though knowledge and treatment of this disease have increased over the years, there is much unknown about BC. One of the topics with little information is the role of the Mast Cell (MC) in the growth and development of cancer. Understanding the role of MC in tumor development can further our understanding of the cancers, leading to drugs that can treat BC better than broad-spectrum chemotherapy. For this study, it was hypothesized that FcεR-1 is expressed but non-functional on the outside of cancer cells *in vitro*.

REVIEW OF THE LITERATURE

Breast Cancer

BC is the second most diagnosed cancer in women in the United States, behind skin cancer. Over the years, advancements in technology and knowledge about BC have increased survival rates among those diagnosed. However, in the United States, it is estimated that 286,600 women will or have been diagnosed with BC in 2021 (American Cancer Society, 2021). Nearly 50,000 of those women have severe enough disease to result in death; this makes BC the second most deadly cancer in the United States, behind lung cancer (American Cancer Society, 2021). The subtype of BC determines prognosis.

a. Triple Negative Breast Cancer

Protein receptors in the extracellular membrane or that reside in the cytosol of tumor cells can help identify the specific subtype of BC the patient was diagnosed with. Triple-negative breast cancer (TNBC) is a form of BC that lacks estrogen receptors (ER), progesterone receptors (PR), and human epidermal growth factor receptor 2 (HER2)

overexpression (Geyer et al., 2017). Due to the decreased presence of these receptors, patients diagnosed with TNBC tend to have lower survival rates overall compared to other subtypes. The absence or under expression of these receptors prevents the use of receptor-targeted treatments.

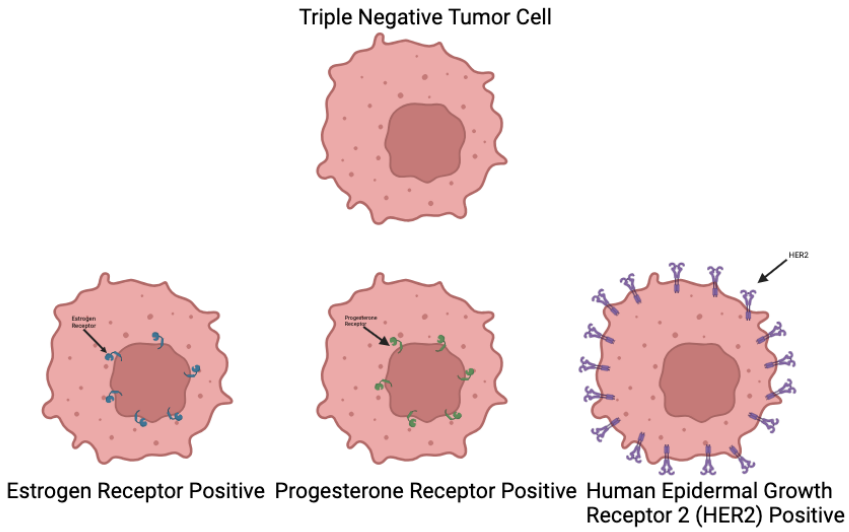

Figure 1 Triple negative BC classification via an absence of ER, PR, and no HER2 overexpression. (made in Bio Render)

b. Luminal-type Breast Cancer

Another form of BC is known as the luminal type. This subtype is also classified into two forms: Luminal A and Luminal B. Luminal A is classified as BC positive for ER and PR within the cell and negative for HER2. Luminal B is classified into two subtypes: luminal B and luminal B-like. Both luminal B subtypes have positive ER, but luminal B is HER2 negative and has minimal PR, and luminal B-like is HER2 positive and has no PR (Inic et al., 2014).

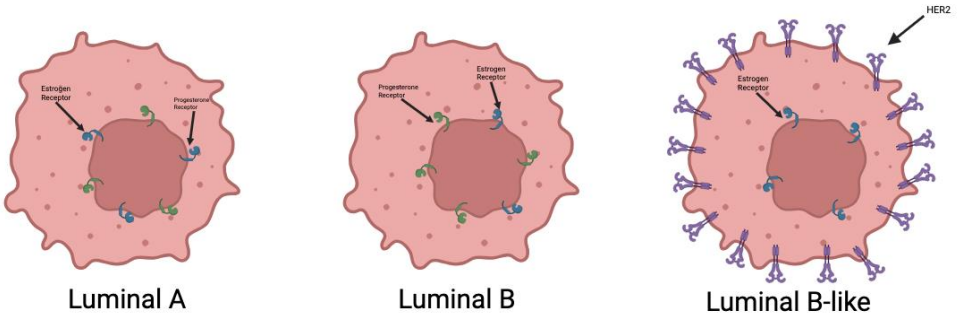

Figure 2 Differences in receptor expression between luminal A (left), luminal B (middle), and luminal B-like (right) (made using Bio Render)

c. HER2-positive breast cancer

The receptor found on mammary tissue cells, known as human epidermal receptor number 2 (HER2), is the receptor used for the average growth and development of the cell (Rubin, Yarden, 2001). The HER2 receptor does not have one specific ligand that binds to create a cellular response but rather multiple ligands (Rubin, Yarden, 2001). This allows growth and development to occur much faster in a malignant cell than in a normal mammary tissue cell. HER2-positive BC cells are cancerous cells with an oversaturation of the HER2 receptor and overexpression of the gene that codes for these receptors (Geyer et al., 2017). Figure 3 shows the difference between a normal cell within the breast tissue and a HER2-positive cancer cell. Since, HER2 is a targetable receptor on the surface of the BC cells, this form of BC can be treated with a medication like Herceptin/HYLECTA.

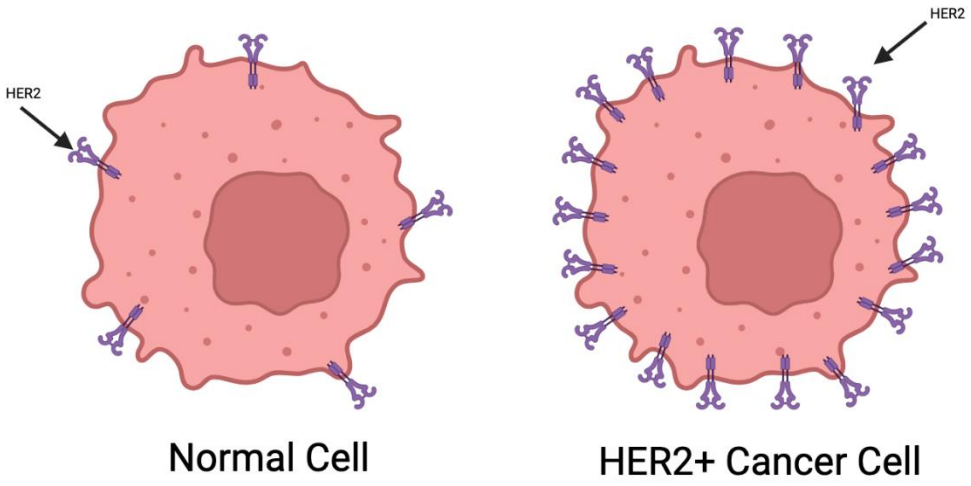

Figure 3 HER2 receptor expression differences between normal cells (left) and HER2+ cancer cells (right) (made using Bio Render)

The Mast Cell

a. What is a Mast Cell?

Mast cells (MC) are immune cells that are now being studied more closely regarding their role in cell growth or death in cancer. Paul Ehrlich first discovered the MC in 1878 during his doctoral thesis work. After his discovery, he hypothesized that these cells were a large part of the microenvironment in connective tissue and aided in feeding neighboring cells. Research has continued since then, and we have learned the MC's role in the immune response to large extracellular invaders (worms) and allergens (Dwyer, Austen, 2021).

When Ehrlich was first working with the MC, he also made note of their presence in tumors. Since he noted their presence, it has been theorized that they infiltrate tumors, one of those being BC tumors. In multiple studies, MCs have been observed to be

protumorigenic, antitumorigenic, and non-important bystanders (Aponte-Lopez et al., 2018).

Most of our knowledge on MC is regarding immune response to allergens, and research continues to observe the effect that MCs have on tumor development in context-dependent studies. There is considerable debate within the immunology community on the role of the MC in cancer development due to the observations of scientists who have reported the MC's ability to switch from pro to anti-inflammatory responses (Galli et al., 2020). A similar observation has been noted when it comes to cancer, the seeming ability for the MC to switch from pro to antitumorigenic properties depending on the type of cancer and the person.

Concerning BC, MCs positive for tryptase, an enzyme released by the MC and a good indicator of MC activation, were in higher concentrations in luminal A and B and less common in TNBC and HER2-positive subtypes (Glajcar et al., 2017). This tryptase-positive MC concentration has been linked to less aggressive cancers and a better outlook due to the suppressive qualities of tryptase in cancer. However, this is counterintuitive because tryptase is associated with allowing fibroblasts and other cells within the tissue to continue to grow, which could, in theory, be more beneficial to cancer cells responding to mitogenic signals (Caughey, G.H., 2008). MCs also contain high levels of histamine, which is mainly associated with allergic reactions. However, BC mouse models have been shown to suppress the immune response, which increases tumor angiogenesis by amplifying the expression of the vascular endothelial growth factor (VEGF) (Majorini et al., 2022). It is expected to see higher proliferation and more aggressive cancers like TNBC and HER2 positive because of the lack of tryptase-positive MCs and the lack of

ER and PR within the cell, allowing for a protumorigenic ECM (Okano et al., 2019). However, the role of MCs in BC development is still controversial.

b. Structure

MCs are round and primarily irregular and filled with granules, small, dense biological organic molecules. These granules are so dense that they often obscure the nucleus from view (Fong, Crane, 2021). When a ligand binds to one of the many IgE receptors around the cell, the MC releases some of these granules into the ECM via exocytosis. The MC then starts to appear flatter and oblong instead of round. This process is called degranulation (Fong, Crane, 2021).

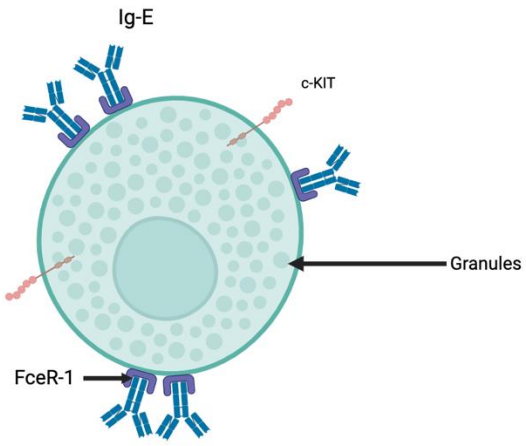

Figure 4 Mast cell structure (made using Bio Render)

i. FcεRI

MCs respond to signals via a high-affinity receptor known as FcεRI. IgE binds to FcεRIα, which triggers a signaling cascade. This cascade starts with the immunoreceptor tyrosine-based activation motifs (ITAMs) located on the β and γ subunits of FcεRI, which causes a phosphorylation cascade and eventual exocytosis of calcium from the endoplasmic reticulum (Kelly et al., 2016).

ii. IgE

Immunoglobulin E (IgE) is produced by allergen-specific B-cells, most often due to an allergic or anti-helminth parasitic stimulus. It is converted into its active IgE form with the help of IL-4 and IL-13 (Kelly et al., 2016). IgE binds to FcεRI without antigen attached to its antigen-binding site. When an antigen does encounter the IgE/FcεRI complex the result is a conformational change in FcεRI that causes signal transduction and degranulation of the MC.

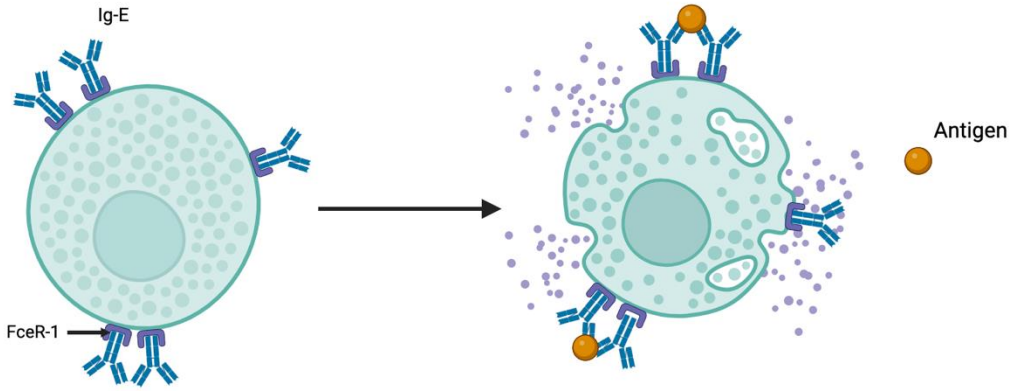

Figure 5 Binding of IgE/antigen complex to FceR-1 causing degranulation of the MC (made using Bio Render).

c. Signaling cytokines

i. Interleukin-6

Interleukin-6 (IL-6) is a cytokine produced by many different cell types like T cells, B cells, monocytes, MC, and some tumor cells. When inflammation increases, IL-6 amplifies by inducing acute phase proteins, increasing angiogenesis and thermogenesis (Fonseca, J.E. et al., 2009). IL-6 is very integrated with the endocrine system, affecting functions positively and negatively. Positively, IL-6 increases the release of growth

hormones and prolactin. On the other hand, IL-6 decreases TSH secretion, which can increase feelings of fatigue, depression, and stress (Tsigos, C. et al., 1997).

Due to the immunomodulatory factors of prolonged IL-6, its role in cancer is of concern. In BC, stromal cells like mesenchymal stem cells, adipocytes, and immune cells have the potential to secrete IL-6 and often will when interacting with cancer cells (Chen, J. et al., 2022). In relation to MCs, IL-6 increases MC proliferation and maturation, allowing for higher reactivity (Desai A. et al., 2016). Furthermore, MC will produce IL-6, which can indicate a potential autocrine loop. Elevated levels of IL-6 in the tumor microenvironment can lead to increased tumor angiogenesis because of the suppression of apoptosis (Chen, J. et al., 2022). Overall, increased levels of IL-6 correlate with lower survival rates in breast cancer patients (Manore S.G. et al., 2022).

ii. Transforming Growth Factor-β

Transforming Growth Factor-β (TGF-β) is a cytokine secreted by epithelial cells and some leukocytes. In cancer, TGF-β has been shown to hinder tumor growth during the initial stages, though as the tumor grows, TGF-β switches roles and aids in the tumor's proliferation (Chaudhury et al., 2009). This cytokine family comprises TGF-β1, 2, and 3 (Travis et al., 2013).

The role of TGF-β operates in a stimulatory and inhibitory fashion in immune cells depending on the environment. In some circumstances, TGF-β will inhibit T cell proliferation by inhibiting IL-2 (Travis et al., 2013). TGF-β will also trigger cell death within T cells after infection (Travis et al., 2013). This effect has been observed during bacterial and viral infections. However, TGF-β in combination with IL-6 is necessary for

healthy immune system development and inflammatory responses for certain T cells (e.g., Th17).

Role of Mast Cells in Breast Cancer

a. Tumor angiogenesis:

MCs are inflammatory cells; elevated levels of inflammation allow for the increase in angiogenesis of tumor cells. Inflammatory cells, like the MC, communicate by signaling pathways; the best example of this is FcεR1, which has a high affinity for binding to IgE, which itself binds to antigen thus causing MC degranulation (Ribatti et al., 2018). The body's vascular structure around the tumor cannot support its growth, which indicates that the tumor has an issue gaining nutrients and removing carbon dioxide from the cells. The tumor increases inflammation by the MC's release of proinflammatory factors like TGF-β, tumor necrosis factor (TNF), and IL-4 (Majorini et al., 2022). Degranulation sends angiogenic factors that start to degrade the matrix around the connective tissue and allow for the formation of new blood vessels around the tumor so it can get more nutrients (Komi et al., 2020). The tumor continues to recruit MCs, which then degranulate and release the TGF-β, TNF, and IL-4, and IL-6 creating a cycle of activation to keep inflammation high to support more and more growth.

b. Tumor growth inhibition:

The potential role of the MC could also be inhibitory to tumor growth. This feature has been noted primarily in BC's luminal A and B subtypes. The recruitment of MCs to areas in high densities alongside a hormonal-based treatment has shown better patient outcomes (Carpenco et al., 2019). Within these subtypes, it has been noted that the high densities of MCs in the tumor microenvironment when degranulated release

chymase and tryptase, the ECM of tumors with both chymase and tryptase had lower proliferation rates (Glajcar et al., 2017).

Significance in Breast Cancer Treatment

MCs are an important part of the immune system, allowing our bodies to fight off invaders effectively. However, they have also been found in the ECM of tumors. Most cancers found with MC in their microenvironment have been linked to prognosis; whether good or bad, this could provide clinicians a unique opportunity to create a more effective treatment. BC is one of these cancers, but there needs to be more consensus within the immunology community on the role of MC in tumor growth and development. This study will observe the effects of MCs, specifically FcεR1, and its role in cell survival within the tumor. FcεR1 is a highly specific receptor to MC and can therefore be a highly targetable for the function of killing cancer cells. The future implications of this study are, with time and other information gathered from other studies, the development of treatments directly targeting the MCs function in the body and within the tumor microenvironment, which can be more effective than chemotherapy.

METHODS AND MATERIALS

Cell Lines

Cell Line	Species	Cell Type
NGS3	Mouse	MC
4T1	Mouse	TNBC
Jurkat	Mouse	T Cell
LAD2	Human	MC
E3	Human	ER^+ BC
EWD8	Human	Basal-like BC
MCF7	Human	ER^+ BC

Table 1: Cell lines used during this study.

Antibodies

Antibody	Vendor	Catalog Number
Alexa Fluor 488 anti-mouse FcεRIα	BioLegend	134330
APC/Cyanine7 anti-human FcεRIα	BioLegend	334631
Purified anti-mouse CD16/32	BioLegend	101302
Human TruStain FcX (Fc block)	BioLegend	422302
Rabbit anti-mouse TGF-βR2 IgG	ABclonal Technologies	A22471
PE Donkey anti-rabbit IgG	BioLegend	406421
PE anti-mouse LAP TGF-β1	BioLegend	141403

Table 2: Antibodies used for this study.

Chloroacetate Esterase Staining (CAE)

CAE staining was done to get a general quantification of MCs in solid tumors. The CAE kit used was the Naphthol AS-D Chloroacetate Esterase Kit from Sigma-Aldrich, Burlington, MA. Tissue sections were cryosectioned between 8-10 μm and stained according to the manufacturer's protocol. In a 15 mL tube, 1 mL of sodium nitrite and 1 mL of the fast red violet LB base solutions were mixed via inversion and allowed to stand for 2 minutes. The solution was then added to 40 mL of DI water warmed to 37°C, 5 mL of TRIZMAL 6.3 buffer concentrate, and 1 mL of Naphthol AS-D Chloroacetate solution. The solution was thoroughly mixed via inversion and turned to a vibrant red color. Room temperature Citrate-Acetone-Formaldehyde solution was used to fix the samples for 30 seconds. Slides were rinsed with DI water for 45 seconds, placed in the Chloroacetate solution, and incubated in the dark for 15 minutes at 37°C. After incubation, the slides were washed with DI water for 2 minutes and then counterstained

in hematoxylin for 2 minutes. The hematoxylin was washed off with tap water, and the slides were allowed to dry before being coverslipped.

Between 8-12 images were taken per section, ensuring that the center and edges for the section were imaged. MCs were quantified, and data was analyzed based on each sample's average number of MCs per high-powered field of view (Lyons, D.O., 2023).

Immunofluorescence

i. FcεRI

The tumors were collected from BALB/cJ mice 28 days after injection with 4T1 cells (Rasé, V.J. et al., 2022). Tumors were frozen at -80ºC until cryosectioned. Sections were cut 8-10 µm thick and stored at -20ºC until stained and analyzed.

The tumor sections were stained with anti-mouse FcεRIα antibody (Table 2). The antibody was diluted with 0.2% Bovine Serum Albumin. Anti-CD-16/32 was used for competitive binding for the FcεRI to avoid non-specific binding to surface Fcγ receptors on the cancer cells. The samples were incubated at 4°C for twenty-four hours. After incubation, the samples were washed with 1X PBS three times. The samples were stained with a 2% Hoechst (nuclei counterstain) solution. The Hoechst was diluted with 1XPBS. This solution was pipetted onto the samples, and the samples were placed in a dark area for thirty minutes. After incubation, the Hoechst was washed off with 1XPBS three times. The samples were cover-slipped and sealed with clear nail polish.

ii. TGF-β

a. TGF-βR2

Tumor sections were stained using Rabbit anti-mouse TGF-βR2 IgG antibody and PE Donkey anti-rabbit IgG antibody (Table 2). The sections were washed with 1X PBS

for 5 min and then air dried. The primary antibody was diluted in 0.2% BSA and incubated on the sections overnight at 4°C. After incubation, the sections were washed with 1X PBS for 5 minutes. The samples were air-dried, stained with the secondary antibody diluted in donkey serum, and incubated for 45 minutes at room temperature. The secondary antibody was washed off with 1X PBS, counterstained with a 2% Hoechst solution, and the coverslipped. Sections were stored at -20°C.

b. TGF-β Latency Associated Peptide (LAP)

Tumor sections were stained using PE anti-mouse LAP TGF-β1 antibody (Table 2). Sections were fixed in a Citrate-Acetone-Formaldehyde solution for 10 minutes and then washed with 1X PBS for 5 minutes. Samples were then placed in a permeabilization solution for 5 minutes. After permeabilization, the samples were washed with 1X PBS for 5 minutes and air-dried. The LAP antibody was added to the sections and incubated overnight at 4°C. The antibody was washed off with 1X PBS for 5 minutes. The sections were counterstained with a 2% Hoechst solution and then coverslipped. The sections were stored at -20°C.

Confocal microscopy

For image capture and analysis, a Zeiss LSM 900 confocal laser scanning microscope and the corresponding software, Zen Blue, were used. Between 12 and 16 images of each sample were taken at 20X or 40X magnification.

Flow Cytometry

All prepared samples were run using the Attune NxT acoustic focusing flow cytometer, and all data were analyzed using FlowJo v.10. Samples were prepped with the following protocol adapted from the BioLegend Cell Surface Flow Cytometry Staining

Protocol. Cells suspended in complete medium (~1x10^6 cells/mL were added to 2 mL Eppendorf tubes and spun down at 350xg for 5 minutes. Media was discarded. Cells were washed twice with cell staining buffer. Supernatant was discarded. Fc block was added to the pellets and left in the fridge for 10 minutes. The antibody and enough cell staining buffer were added to bring the total volume to 100 µL. The samples were incubated in the fridge for 20 minutes. The volume of the tubes was raised using cell staining buffer (~600 µL). Samples were centrifuged at 350xg for 5 minutes. The supernatant was discarded, and samples were washed twice using a cell staining buffer. The supernatant was discarded, and the samples were resuspended in 1 mL of cell staining buffer.

i. FcεRI

The cells used for this assay were 4T1, NGS3s, E3s, EWD8s, MCF7s, and LAD2s (Krishenbaum, A.S et al., 2003)—cells grown *in vitro.* Approximately one million cells were analyzed per sample and stained using the FcεR-1α and Fc block antibodies listed in Table 2.

ii. Ca^{2+} Flux Assay

The Ca^{2+} Flux Assay is a method to assess the degranulation potential of mast cells using a flow cytometer. This assay was done with BMMCs and 4T1s to test the functionality of FcεRI. The cells are sensitized with TNP-KLH (antigen)-specific IgE for twenty-four hours at a 0.5 µg/mL concentration. Fluo-4 AM – the Ca^{2+} fluorescent indicator – is dissolved in DMSO at a concentration of 1 mM. Before the Fluo-4 AM was added to the cells, the cells were centrifuged at 350xg for 5 minutes, and the supernatant was discarded. Cells were washed twice with calcium-free PBS. Fluo-4 AM was added at 1 µM per 1X10^7 cells/mL. The cells are then incubated for 45 minutes at 37ºC. After

incubation, cells were washed with PBS and allowed to rest for 30 minutes at room temperature. Flow was run initially without antigen to obtain a calcium baseline for 60 seconds. The tube was removed from the flow cytometer and 1 µL of TNP-KLH was added, the lid was closed, sample was mixed via inversion. The tube was quickly placed back on the flow cytometer, and data was collected again for another 60 seconds to see a change in extra-calcium concentration (protocol based on Vita, A.A. and Pullen, N.A, 2022). NGS3s and 4T1s calcium indicator used was Fluo-4 AM from Invitrogen Waltham, MA. LAD2, EWD8, E3s, and MCF7s calcium indicator was ICR-1 AM from Ion Biosciences San Marcos, TX.

Polymerase Chain Reaction (PCR)

PCR was used to determine the presence of αβγ subunits, using DNA primers designed to target specific subunits. Primers were crosslinked for human and mouse FcεR-1 (Table 3).

Primer Name	5'-3'	Primer Length	TM (°C)
FcεR-1α-F	ACTGTACGGGCAAAGTGTGG	81	60.53
FcεR-1α-R	ACTTCTCACGCGGAGCTTTT	81	60.25
FcεR-1β-F	CCTCCAGTGCACCTGACATT	149	59.96
FcεR-1β-R	ATGTCCGCCATGTCTGCTTT	149	60.32
FcεR-1γ-F	GCCGTGATCTTGTTCTTGCTC	78	59.87
FcεR-1γ-R	GCCTTTCGGACCTGGATCTT	78	59.75

Table 3: FceR-1 PCR Primer Sequences

a. RNA Extraction

The total RNA was extracted using the TRIzol Plus RNA Purification Kit from Invitrogen Waltham, MA. Cell samples were lysed and centrifuged to separate phases with the liquid phase containing RNA according to the manufacturer's protocol. RNA was washed and eluted into an Eppendorf tube. Purity was measured with the NanoDrop Spectrophotometer.

RNA without adequate concentrations (lower than 100 ng/μL) and purities (a 260/280 ratio less than 1.5) were further purified; samples were reconstituted in a small volume of liquid. This was done by adding 0.1X volume of 3M sodium acetate (pH 5.2) to the samples, then adding cold 100% ethanol and cold isopropanol. Tubes were inverted to mix and then placed on ice for 10 minutes. RNA samples were centrifuged at 14,000xg at 4°C for 10 minutes. The supernatant was carefully removed, and the pellets were washed with 1000μL of 75% ethanol. Samples were centrifuged again for 2 min (same settings as before). The supernatant was removed, and the samples were centrifuged once more for 1 minute. Any excess supernatant was removed. The pellets were air-dried with the Eppendorf tube caps left open for 3 minutes. The pellets were resuspended with 15μL of nuclease-free water. Purity and concentration were checked once more using the NanoDrop Spectrophotometer.

b. cDNA synthesis

This was completed using the QuantiTect Reverse Transcription Kit (Cat. No. 205311) from Qiagen Germantown, MD. cDNA was made from the RNA samples from all cell lines in a 20μL volume reaction with 1 μg of total RNA for each cell line. In 0.2 mL nuclease-free PCR tubes, 1μL dNTPs and 1μL anchored oligo dT22 were added and adjusted with water for a total volume of 13 μL. The samples were placed in the thermal

cycler at 65°C for 5 minutes, then a 12°C hold. The RNA was placed on ice to allow for denaturation. Then, 4 μL 5X First-strand buffer, 1.2 μL DEPC-treated water, 1 μL DTT, 0.5 μL RNase OUT (Invitrogen 10777-019), and 0.3 μL SuperScript III were added for a total volume of 20 μL. Samples were placed in the thermocycler once more programmed at 25°C for 5 min, 50°C for 1 hour, 70°C for 15 minutes, and 12°C hold. Samples were stored at -80°C until ready for PCR.

c. PCR

The PCR kit used was the QuantiTect SYBR Green PCR Kit (Cat. No. 204163) from Qiagen Germantown, MD. Primers was purchased from Invitrogen Waltham, MA. Primers were diluted in nuclease-free water for a concentration of 2 μM. Each tube contained 10 μL MasterMix 1 μL forward primer, 1 μL reverse primer, and 8 μL cDNA per cell line. Samples were loaded into the thermocycler and programmed for 1 cycle of 94°C for 2 minutes (initial denaturation), 40 cycles of denaturation at 94°C for 30 seconds, annealing at 55°C for 30 seconds, and elongation at 72°C for 30 seconds, followed by a 10-minute extension for final elongation at 72°C, and finally a 12°C hold.

d. Gel Electrophoresis

A 2% agarose gel was prepared. Samples were prepared for the gel by combining 3.3 μL 6X SYBR Green, 4.7 μL nuclease-free water, and 12 μL PCR samples. The samples were loaded along with a 1Kb GeneRuler Plus DNA ladder from Thermo Fisher Scientific Waltham, MA. Gel was run in 1X TAE at 100 V until adequate band separation was achieved (about 1 hour).

IL-6 Enzyme-Linked Immunosorbent Assay (ELISA)

This assay was done with the Human IL-6 ELISA Max Deluxe Set from BioLegend San Diego, CA, following the manufacturer's protocol. First, diluted capture antibody at a concentration of 0.5 μg/mL, was dispensed at 100 μL in each well of a flat bottom 96-well plate. The plate was covered and incubated at room temperature overnight. After the overnight incubation, the plate was washed with wash buffer (0.05% Tween-20 in 1X PBS), and the 200 μL of block buffer (0.5% BSA in 1X PBS) should be added to the wells and incubated at room temperature for 1 hour. The plate was washed, and 100 μL of the samples and standard curve solutions were added to the wells and incubated at room temperature for 2 hours. The plate was washed, and the detection antibody was added at a concentration of 0.5 μg/mL at a volume of 100 μL/well and incubated at room temperature for 1 hour. The plate was rewashed, and the Avidin HRP was added to each well (100 μL/well) and incubated for 30 minutes. The Avidin was washed off, and the TMB substrate was added to each well (100 μL/well). The data was collected immediately using the SpectraMax 190 microplate reader. The data was analyzed using the GraphPad Prism 10 software.

Mouse IL-6 ELISA Max Deluxe Set from Peprotech Inc. Cranbury, NJ, was completed similarly to the Human IL-6 ELISA steps above.

R-2 Genomic Data Search

The genetic database R2: Genomics Analysis and Visualization Platform (http://r2platform.com) was used to apply the data collected with the *in vitro* models within this study to human tissue removed from patients. The genes GAPDH, ACTB, FcεR-1α, and TGF-β1 were searched on the tissue expression data in Table 4.

Author	Tissue Type	Sample Size
Belitskaya-Levy	Postmenopausal Normal Breast	107
Russo	Nulli-parous Normal Breast	113
Russo	Full-term Pregnancy Normal Breast	109
Gruvberger-Saal	Primary Tumor Breast	3207
Brown	TNBC Tumor Breast	198
Sinn	Tumor Breast Metastatic	1108

Table 4: R2 genomic tissue samples

RESULTS AND DISCUSSION

Chloroacetate Esterase Staining

Chloroacetate Esterase (CAE) is a staining method that stains MC granules magenta/pink while other cells are stained purple. This staining technique was first to the tumor samples, and it was found that the IL-6 KO tumors had a higher concentration of MCs compared to the WT control tumors (Lyons, D.O., 2023). The immunofluorescent staining was done to get data of cells that express FcεRI, which allowed for the capture of other cells expressing this receptor and not just MCs.

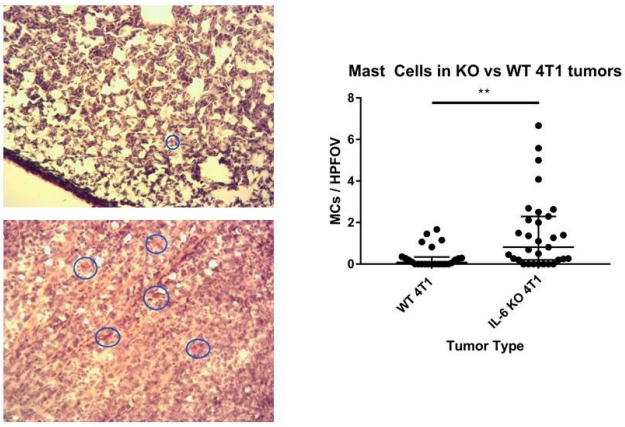

Figure 6: Left: Images of CAE staining. Top: WT 4T1 tumors. Bottom: 1L-6 KO tumors. Right: Quantification of the MC concentration between WT and KO tumors. KO tumors are significantly more likely to have higher MC counts (p<0.05). (From Lyons, D.O., 2023)

FcεRI Fluorescence

Intense FcεR-1 staining was noticed for the IL-6 knockout sections, more so compared to the wild-type. A few possible reasons exist for a large portion of positive staining within the tumor samples. The tumor contains many MCs, or other cells that express the FcεR-1 receptor. In the WT 4T1 tumors, a fibrous capsule surrounded the tumor where the mast cell concentration was the highest; this was not seen in the IL-6 KO tumors.

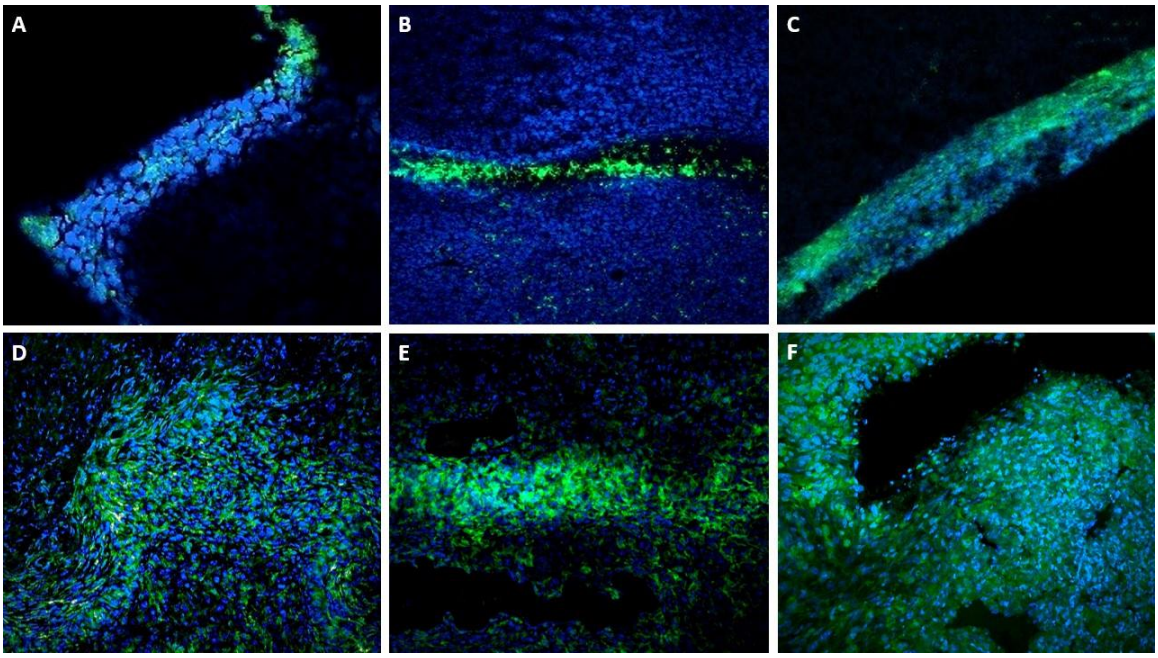

Figure 7: A-C Control "Wildtype" 4T1 tumors stained for FcεRI (green) and Hoechst (blue) at 20X magnification. D-F: IL-6 knock-out 4T1 tumors stained for FceR-1 (green) and Hoechst (blue) 20X magnification. All images were taken with the Zeiss LSM-900 microscope.

TGF-β Fluorescence

a. TGF-βRII Staining

Since TGF-β switches from anti-inflammatory to proinflammatory once a tumor has been established to aid in tumor proliferation (Chaudhury et al., 2009), the expression of the receptor, TGF-βRII, was measured by looking for a difference between the WT and KO tumors. It was hypothesized that the IL-6 KO would have a higher expression of TGF-βRII compared to the WT, like what was seen for the anti-FcεR-1 fluorescent staining. There is a very slight difference between WT and IL-6 KO. It does appear that the WT tumors express more TGF-βRII compared to the KO because of the redder tone of the images, indicating more red staining from the TGF-βRII antibody, while the KO has more of a purple tone due to less positive TGF-βRII staining meaning the blue of the Hoechst is more apparent (Figure 7). This higher expression of TGF-βRII in the WT 4T1

tumors was an unexpected result. Studies have shown that compared to noncancerous tissue, there is an upregulation of TGF-βRII within colorectal cancer (Gatza C.E. et al., 2011). It would be worth comparing these results to noncancerous mammary tissue and comparing the differences.

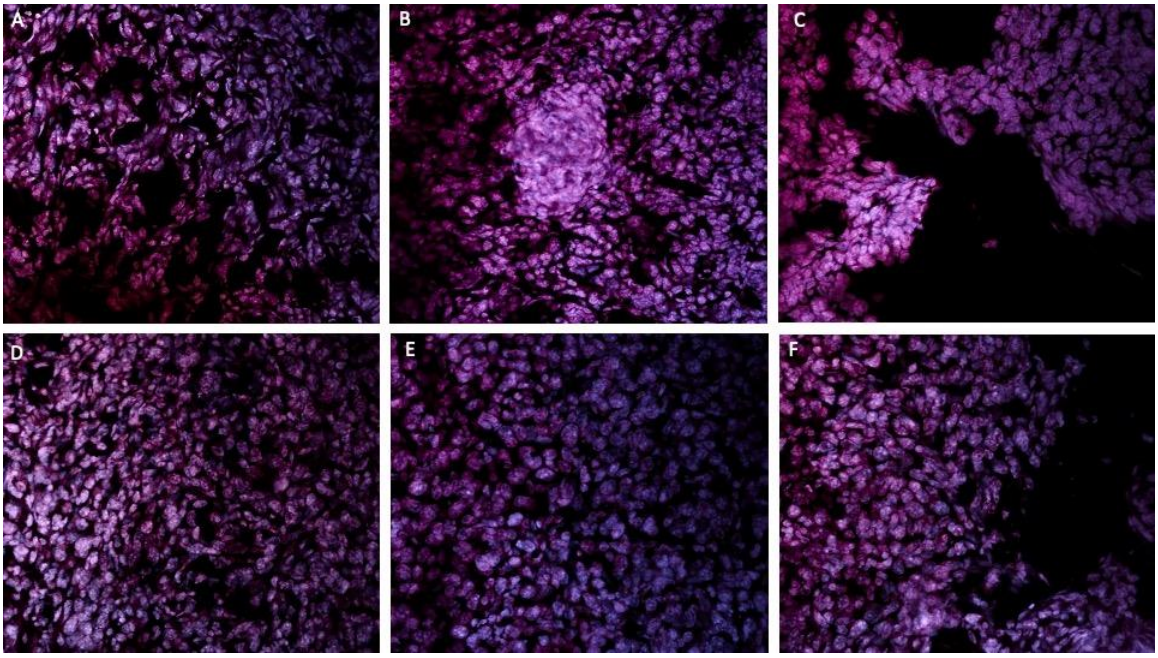

Figure 8: A-C 4T1 WT tumor sections stained with TGF-RII (red) and counterstained with Hoechst (blue). D-F: IL-6 knock-out 4T1 tumors stained with TGF-RII (red) and counterstained with Hoechst (blue). All images were taken at 20X magnification.

b. TGF-β LAP Staining

A cell increasing the expression of a receptor would also correlate to an increase in that receptor's ligand; the higher expression of TGF-β LAP in the WT was expected after seeing a higher expression of TGF-βRII in the WT compared to the KO (Figure 8).

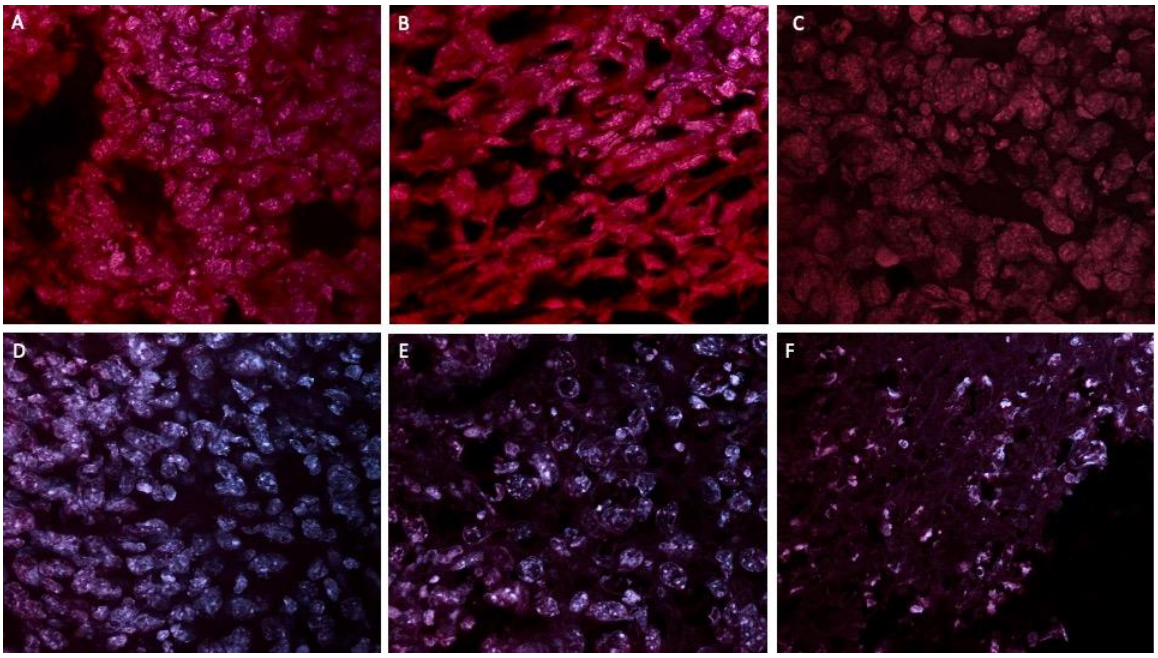

Figure 9: A-C: 4T1 WT tumors stained with TGF-β LAP antibody (red) and counterstained with Hoechst (blue) at 40X magnification. D-F: 4T1 IL-6 KO tumors stained for TGF-β LAP (red) and counterstained with Hoechst at 40X magnification.

When comparing these data to the FcεR1 images, it is seen that these two receptors are inversely expressed, with more TGF-βRII expressed in the WT and more FcεR1 expressed in the KO tumors, which implies that an absence of IL-6 less TGF-β is produced in the tumor microenvironment. This phenomenon was also seen in the R2 genomics search, with FcεR-1 being downregulated in the tumor and TGF-βRII being upregulated.

Anti-FcεRIα Expression

To understand the reason for high concentrations of positive FcεR1 staining within solid tumor sections, an *in vitro* assay was done using the same FcεR1α antibody used in the confocal microscopy. This assay showed a positive result for NGS3 BMMCs and 4T1s but negative for Jurkats, a mouse T-cell leukemia cell line. The positive BMMCs and negative Jurkats were expected, though the positive 4T1s were unexpected.

A CD16/32 block was used to ensure specificity to FcεR1. This expression in the 4T1 cells has not been noted in the literature.

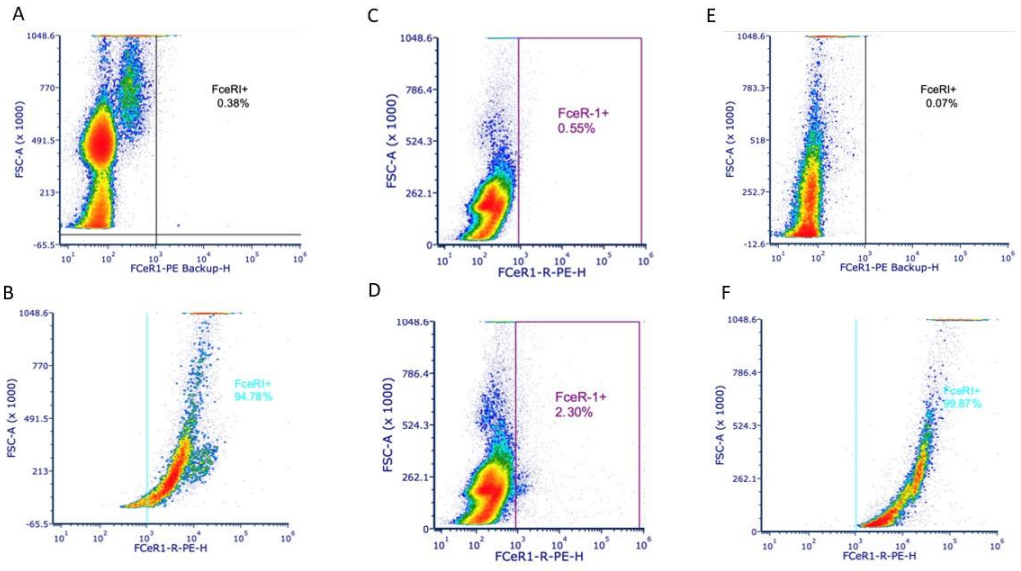

Figure 10: A- Unstained negative control C57BL/6J BMMCs. B-Stained BMMCs for anti-mouse Fc□R1,>90% positive, as expected. C- Unstained negative control Jurkat. D-Stained Jurkat for anti-mouse Fc□R1. E- Unstained negative control 4T1s. F-Stained 4T1s for anti-mouse FcεRI >90%, an unexpected result.

This assay was repeated with human LAD2, E3, EWD8, and MCF7 cells. The results were mostly consistent with the data collected with the mouse cells. The LAD2s were used as a positive control and expressed FcεR1 as expected. The three cancer cell lines expressed FcεR1. The EWD8s basal-like cell line expressed a similar amount of FcεR1, ~76% positive. This was an unexpected result. The E3s and MCF7 cell lines expressed a smaller amount of FcεR-1, ~33% and ~11%, respectively (Figure 10). Both cell lines are ER+ luminal-like BC, which tends to be less aggressive than the basal-like EWD8 cell line (Haughian JM et al., 2011). This is a possible explanation for the difference in FcεR1 expression. The literature has not noted this expression of FcεRI on human-immortalized cell lines.

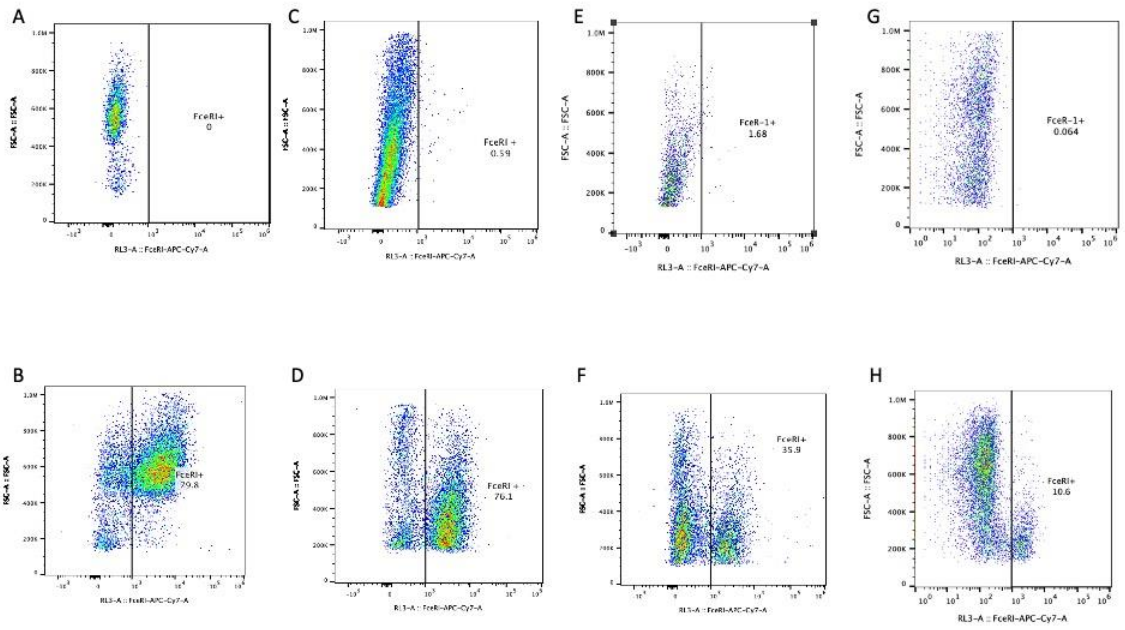

Figure 11: A. Unstained negative control LAD2. B.-Stained LAD2s for anti-human FcεR-1, ~80% positive as expected. C. unstained negative control EWD8s. D. Stained EWD8s for anti-human FcεR1, ~76% positive, an unexpected result. E. Unstained negative control E3s. F. Stained E3s for anti-human FcεR1, ~36% positive, an unexpected result. G. Unstained negative control MCF7s. H. Stained MCF7s for anti-human FcεR1, ~11% positive, an unexpected result.

Ca^{2+} Assay

Calcium can be used to measure the early activation function of FcεR1. Crosslinking of the receptor via IgE + antigen causes release of calcium from the endoplasmic reticulum, which is critical for degranulation and can even exit to the ECM (Nagata, Y. & Suzuki, R., 2022). In the mouse model, as expected, the MCs (NGS3s) had an increased calcium release from the ER into the ECM after adding antigen. The cancer cells did not, with the 4T1s starting low and increasing before and after antigen addition.

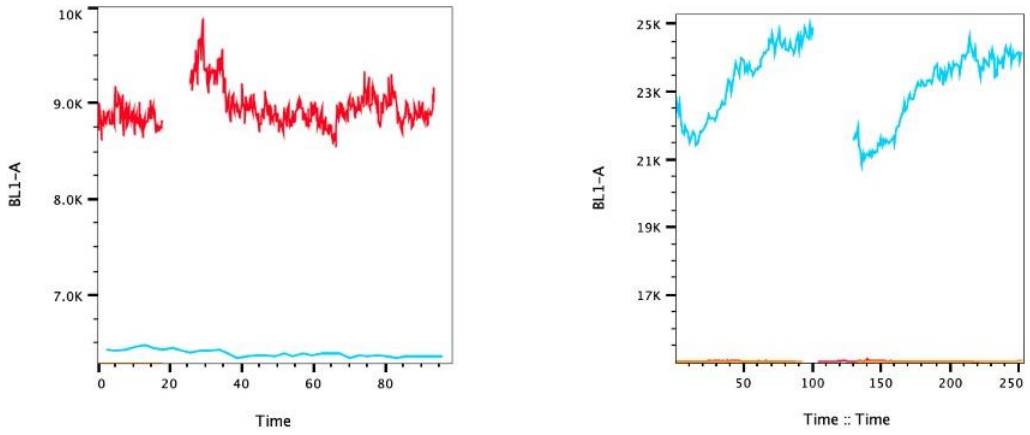

Figure 12: Mouse Ca^{2+} Assay. Left: NGS3 Ca^{2+}, Red: NGS3s, +IgE, +Fluo-4AM. Blue: NGS3s, +IgE, -Fluo-4AM. Orange: NGS3, -IgE, -Fluo-4AM. NGS3s, after activation with TNP-KLH, had an increase of Ca^{2+} as expected (red). Right: 4T1 Ca^{2+} Assay. Blue: 4T1, +IgE, +Fluo-4AM. Orange: 4T1, +IgE, -Fluo-4AM. Red: 4T1, -IgE, -Fluo-4AM. 4T1s did not have a difference in Ca^{2+} release post activation with TNP-KLH.

In the human model, the LAD2s released calcium from the ER after adding antigen, as expected. The E3s and EWD8s started at lower calcium levels after antigen addition than those without antigen stimulation before increasing slowly. The MCF7s did not show an increase in calcium after adding the antigen.

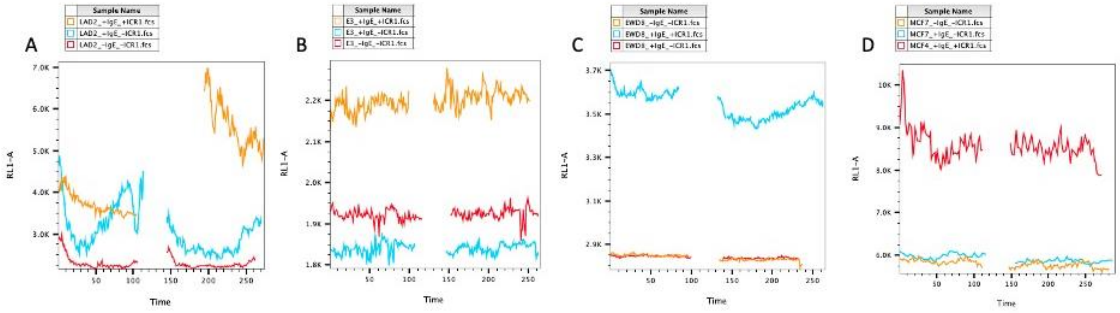

Figure 13: Human Ca^{2+} Assay. A: LAD2 Ca^{2+} B: E3 Ca^{2+} C: EWD8 Ca^{2+} D: MCF7 Ca^{2+} LAD2s showed an increase in Ca^{2+} after the addition of antigen, as expected. E3, EWD8s, and MCF7s did not show any change in Ca^{2+} post antigen stimulation.

PCR

Determining the presence of the αβγ subunits within the 4T1s, E3s, EWD8s, and MCF7s is an important step in understanding the function of FcεR1 within these cells. The NGS3s expressed all three subunits (αβγ) as expected. Though the γ subunit in the

NGS3 showed two bands, the reason for this is unknown and could be a mutation derived from when the cells were immortalized (Figure 13). The 4T1s also expressed all three subunits (αβγ), which was unexpected. The β band was also brighter in the 4T1 than the β band of the NGS3s, which could indicate that the 4T1s produce more of this subunit than the NGS3. The expression of the αβγ subunits indicates that these cells are using this receptor for some function.

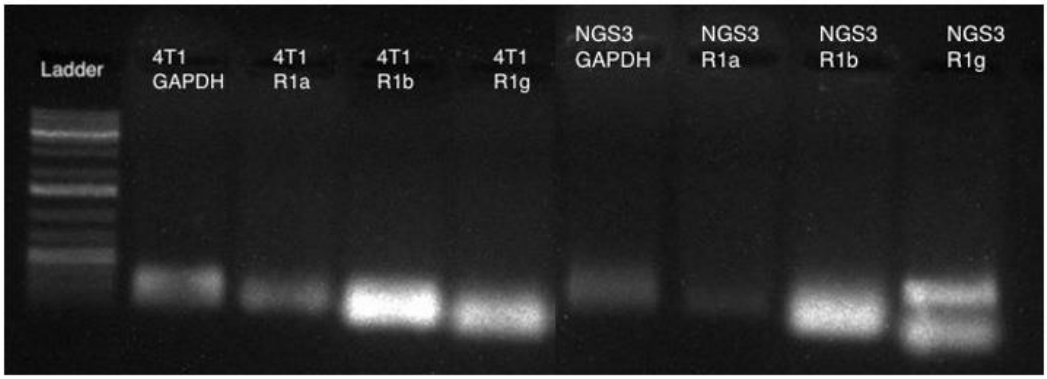

Figure 14: PCR gel from 4T1 and NGS3s. NGS3s expressed all three subunits (□□□) as expected, and the 4T1s expressed all three subunits (□□□), which was an unexpected result.

The E3s, EWD8s, and MCF7s also express all three subunits (αβγ). The brighter β band in the E3s and EWD8s means a potentially higher concentration of this subunit than the αγ subunits. The MCF7 band appear to not express any of the subunits of FcεRI and the results see are most likely primer dimers.

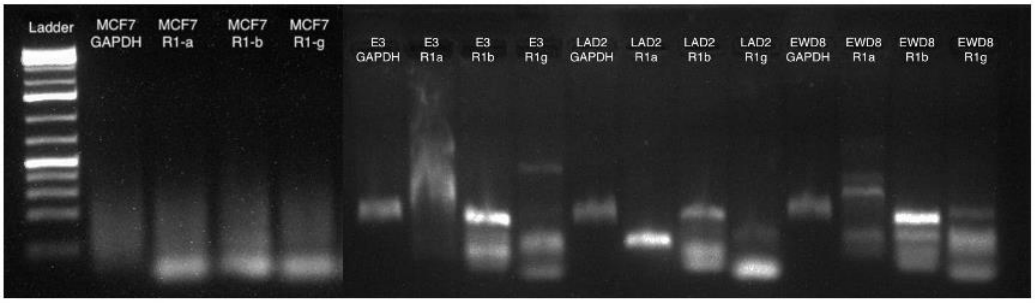

Figure 15: LAD3, E3, EWD8, and MCF7s PCR gel. LAD2s expressed all three subunits as expected. E3s and EWD8s expressed all three subunits: an unexpected result. MCF7s did not express any of the subunits.

IL-6 ELISA

Activation of FcεR1 with IgE and antigen (TNP-KLH) will lead to the upregulation and release of IL-6 from MC (Fonseca, J.E. et al., 2009). The ELISA measured the concentration of IL-6 in the medium after activation with IgE and TNP-KLH after 24 hours to measure the function of the FcεR1. The NGS3s increased the amount of IL-6 after IgE and TNP-KLH activation, though once there was too much stimulation with antigen, IL-6 concentration decreased as expected. The 4T1s did not produce and subsequently release any IL-6 at any concentration of TNP-KLH antigen. This, along with calcium indicator data, indicates that the receptor is nonfunctional in the 4T1 cells despite microscopy and flow data observing FcεRI protein and the PCR results indicating all three subunits are transcribed. Looking further down in the signaling pathway to determine the difference would allow a better understanding of why/how FcεR1 is present on these cells and its overall function.

The human cell lines had a different result. The LAD2s produced and released small amounts of IL-6 when stimulated with IgE and TNP-KLH. The concentration of IL-6 also decreased slightly at the high dose of antigen. This was expected, but typically, MC releases more IL-6 at low dose antigen than was observed here. Though this is a cancerous cell line, it can be assumed that they produce lower amounts of IL-6. Another

interesting observation is that the EWD8s and the E3s produced IL-6, which was unexpected. The EWD8s produced IL-6 with stimulation with IgE and with IgE and antigen. The E3s acted similarly to the LAD2s, with the IL-6 being created after the simulation of IgE and antigen and decreased concentration at the high antigen dose (Figure 15). The MCF7s did not produce any IL-6.

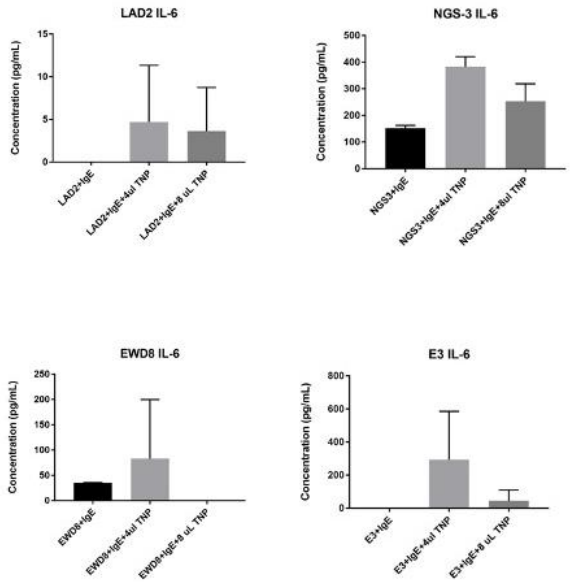

Figure 16: IL-6 ELISA results. LAD2 & NGS3s produced IL-6 as expected with give IgE and antigen. E3s and EWD8s also produced IL-6 which was an unexpected result. 4T1s and MCF7s did not produce any IL-6 (not pictured).

R2 Genomics

Of the six genomic data sets examined, three being normal breast tissue and three being tumor tissue, there was an overall trend between normal and cancerous: FcεR1 is downregulated in a tumor compared to normal tissue. TGF-β is up-regulated in a tumor, consistent with the class switch effect we see in cancer (Chaudhury et al., 2009). FcεR1 being downregulated is an interesting result because it is the opposite of what we see in immortalized cell lines that are commonly used to study BC. This result shows a

difference between primary tissue removed from a human patient and the assays done with immortalized human cell lines.

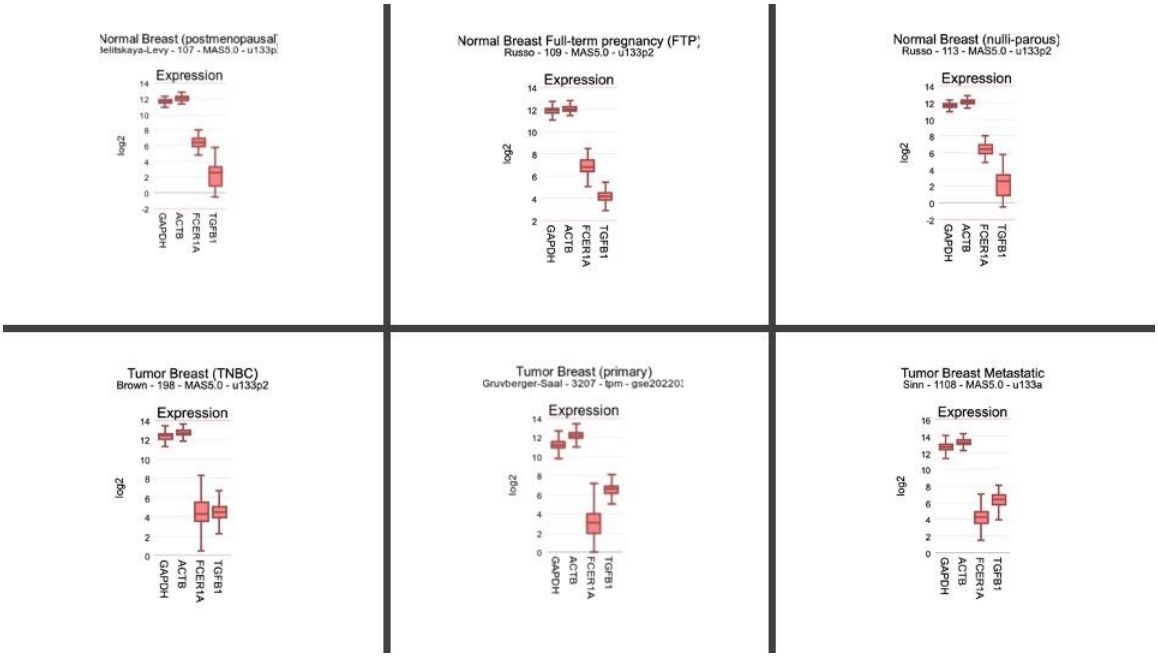

Figure 17: R2 Genomics search results. Top row: normal breast tissue. Bottom row: tumor breast tissue.

CONCLUSION

The observations within this research project have noted that: (1) MC traffic to mammary carcinoma that is IL-6 deficient *in vivo* (in a mouse 4T1 model); (2) that upon further analysis, 4T1 tumors abundantly express FcεRI, TGF-β, and TGF-β receptor; (3) 4T1 cells and other human breast cancer cell lines abundantly express FcεRI *in vitro*; (4) that the function of FcεRI is limited to cytokine production only in some cell line *in vitro*; and (5) that conversely to cell models, primary human breast cancers do not express more or less FcεRI than primary non-cancerous breast tissue. Importantly, the functionality tests run during this study showed that FcεR1 is nonfunctional in BC models in a traditional sense with respect to MC; to determine function in these cell lines, we would need to examine the signaling pathway of FcεRI in more detail. However, within human

breast cancer tissue, FcεR1 expression is downregulated, which means the issue with these cells expressing this receptor could be that they are immortalized, and thus FcεRI expression is an artifact of their natural history that is irrelevant to the real human pathology. A mutation likely developed by the cells when they were initially immortalized. Interestingly, all the examined BC lines produced this (perhaps except MCF7), which could indicate another common route to aberrant protein expression in cell lines that might be of future interest. Regardless, these cells should be used cautiously if studying the interaction between BC and MCs within the tumor microenvironment. This caveat is particularly important in the context of 4T1 cells since these are also used as an immunocompetent *in vivo* BC model in Balb/c mice. These observations also bring for a call to examine the associations and roles of MC more intentionally in primary human breast tissue as well as primary human BC. FcεRI remains a relatively unique surface target for MC that can be leveraged therapeutically if MC make any deleterious contributions to the BC microenvironment.

REFERENCES

Aponte-López, A., Fuentes-Pananá, E. M., Cortes-Muñoz, D., & Muñoz-Cruz, S. (2018). Mast Cell, the Neglected Member of the Tumor Microenvironment: Role in Breast Cancer. *Journal of Immunology Research, 2018*, 2584243-11. 10.1155/2018/2584243

Banafea, G. H., Bakhashab, S., Alshaibi, H. F., Natesan Pushparaj, P., & Rasool, M. (2022). The role of human mast cells in allergy and asthma. *Bioengineered*, *13*(3), 7049–7064. https://doi.org/10.1080/21655979.2022.2044278

Belitskaya-Levy. (2023). R2 Genomics Analysis and Visualization Platform [Dataset]. In *Expression data from breast samples of postmenopausal women*. https://hgserver1.amc.nl/cgi-bin/r2/main.cgi

Brown. (2016). R2 Genomics Analysis and Visualization Platform [Dataset]. In *Comprehensive genomic analysis identify novel subtypes and targets of triple-negative breast cancer*. https://hgserver1.amc.nl/cgi-bin/r2/main.cgi

Carpenco, E., Ceauşu, R. A., Cimpean, A. M., Gaje, P. N., Șaptefraţi, L., Fulga, V., David, V., & Raica, M. (2019). Mast Cells as an Indicator and Prognostic Marker in Molecular Subtypes of Breast Cancer. *In vivo (Athens, Greece)*, *33*(3), 743–748. https://doi.org/10.21873/invivo.11534

Caughey G. H. (2007). Mast cell tryptases and chymases in inflammation and host defense. *Immunological reviews*, *217*, 141–154. https://doi.org/10.1111/j.1600-065X.2007.00509.x

Chaudhury, A., & Howe, P. H. (2009). The tale of transforming growth factor-beta (TGFbeta) signaling: a soigné enigma. *IUBMB life*, *61*(10), 929–939. https://doi.org/10.1002/iub.239

Chen, J., Wei, Y., Yang, W., Huang, Q., Chen, Y., Zeng, K., & Chen, J. (2022). IL-6: The Link Between Inflammation, Immunity, and Breast Cancer. *Frontiers in oncology*, *12*, 903800. https://doi.org/10.3389/fonc.2022.903800

Collignon, J., Lousberg, L., Schroeder, H., & Jerusalem, G. (2016, May 20). *Triple-negative breast cancer: Treatment challenges and solutions*. Breast cancer (Dove Medical Press). Retrieved February 14, 2022, from https://www.ncbi.nlm.nih.gov/pmc/articles/PMC4881925/

Constantine Tsigos, Dimitris A. Papanicolaou, Ruby Defensor, Constantine S. Mitsiadis, Ioannis Kyrou, George P. Chrousos; Dose Effects of Recombinant Human lnterleukin-6 on Pituitary Hormone Secretion and Energy Expenditure. *Neuroendocrinology* 1 January 1997; 66 (1): 54–62. https://doi.org/10.1159/000127219

Desai, A., Jung, M. Y., Olivera, A., Gilfillan, A. M., Prussin, C., Kirshenbaum, A. S., Beaven, M. A., & Metcalfe, D. D. (2016). IL-6 promotes an increase in human mast cell numbers

and reactivity through suppression of suppressor of cytokine signaling 3. *The Journal of allergy and clinical immunology*, *137*(6), 1863–1871.e6. https://doi.org/10.1016/j.jaci.2015.09.059

Dwyer, D. F., & Austen, K. F. (2021). The discovery of discrete developmental pathways directing constitutive and induced mast cells in mice. *The Journal of Immunology*, *207*(2), 359–361. https://doi.org/10.4049/jimmunol.2100432

Haughian JM; Pinto MP; Harrell JC; Bliesner BS; Joensuu KM; Dye WW; Sartorius CA; Tan AC; Heikkilä P; Perou CM; Horwitz KB; (2011, October 3). *Maintenance of hormone responsiveness in luminal breast cancers by suppression of notch*. Proceedings of the National Academy of Sciences of the United States of America. Retrieved May 4, 2023, from https://pubmed.ncbi.nlm.nih.gov/21969591/

Ellis, R. (n.d.). *Hematoxylin and Eosin (H&E) Staining Protocol*. Hematoxylin and eosin (HE) staining protocol. Retrieved December 5, 2021, from http://www.ihcworld.com/_protocols/special_stains/h&e_ellis.htm.

Fong, M. (2021, May 10). *Histology, Mast Cells*. StatPearls [Internet]. Retrieved November 27, 2021, from https://www.ncbi.nlm.nih.gov/books/NBK499904/.

Fonseca, J.E., Santos, M.J., Canhao, H., and Choi, E., (2009). Interleukin-6 as a key player in systemic inflammation and joint destruction. *Autoimmunity Reviews, 8(7),* 538-542. https://doi.org/10.1016/j.autrev.2009.01.012

Frozen section protocol. Frozen Section Protocol | Sino Biological. (n.d.). Retrieved December 5, 2021, from https://www.sinobiological.com/category/frozen-section-protocol.

Galli, S. J., Gaudenzio, N., & Tsai, M. (2020). Mast cells in inflammation and disease: Recent progress and ongoing concerns. *Annual Review of Immunology, 38*(1), 49–77. https://doi.org/10.1146/annurev-immunol-071719-094903

Gatza, C. E., Holtzhausen, A., Kirkbride, K. C., Morton, A., Gatza, M. L., Datto, M. B., & Blobe, G. C. (2011). *Type III TGF-β receptor enhances colon cancer cell migration and anchorage-independent growth.* Neoplasia (New York, N.Y.), 13(8), 758–770. https://doi.org/10.1593/neo.11528

Geyer, F. C., Pareja, F., Weigelt, B., Rakha, E., Ellis, I. O., Schnitt, S. J., & Reis-Filho, J. S. (2017, October). *The spectrum of triple-negative breast disease: High- and low-grade lesions*. The American journal of pathology. Retrieved November 12, 2021, from https://www.ncbi.nlm.nih.gov/pmc/articles/PMC5809519/.

Glajcar, A., Szpor, J., Pacek, A., Tyrak, K. E., Chan, F., Streb, J., Hodorowicz-Zaniewska, D., & Okoń, K. (2017, May). *The relationship between breast cancer molecular subtypes and*

mast cell populations in tumor microenvironment. Virchows Archive: an international journal of pathology. Retrieved November 12, 2021, from https://www.ncbi.nlm.nih.gov/pmc/articles/PMC5406445/.

Green, D. P., Limjunyawong, N., Gour, N., Pundir, P., & Dong, X. (2019, February 6). A mast-cell-specific receptor mediates neurogenic inflammation and pain. Neuron. Retrieved February 5, 2022, from https://www.ncbi.nlm.nih.gov/pmc/articles/PMC6462816/.

Gruvberger-Saal. (2022). R2 Genomics Analysis and Visualization Platform [Dataset]. In Clinical associations of ESR2 (estrogen receptor beta; ERÎ²) expression across thousands of primary breast tumors. https://hgserver1.amc.nl/cgi-bin/r2/main.cgi

How common is breast cancer? Breast cancer statistics. American Cancer Society. (n.d.). Retrieved November 11, 2021, from https://www.cancer.org/cancer/breast-cancer/about/how-common-is-breast-cancer.html.

Immunocytochemistry and immunofluorescence Staining Protocol. Abcam. (2021, November 18). Retrieved December 5, 2021, from https://www.abcam.com/protocols/immunocytochemistry-immunofluorescence-protocol.

Inic, Z., Zegarac, M., Inic, M., Markovic, I., Kozomara, Z., Djurisic, I., Inic, I., Pupic, G., & Jancic, S. (2014, September 11). *Difference between Luminal A and luminal B subtypes according to Ki-67, tumor size, and progesterone receptor negativity providing*

prognostic information. Clinical Medicine Insights. Oncology. Retrieved November 12, 2021, from https://www.ncbi.nlm.nih.gov/pmc/articles/PMC4167319/.

Kelly, B. T., & Grayson, M. H. (2016). Immunoglobulin E, what is it good for? *Annals of Allergy, asthma & immunology: official publication of the American College of Allergy, Asthma, & Immunology*, *116*(3), 183–187. https://doi.org/10.1016/j.anai.2015.10.026

Kirshenbaum, A. S., Akin, C., Wu, Y., Rottem, M., Goff, J. P., Beaven, M. A., Rao, V. K., & Metcalfe, D. D. (2003). Characterization of novel stem cell factor responsive human mast cell lines LAD 1 and 2 established from a patient with mast cell sarcoma/leukemia; activation following aggregation of FcepsilonRI or FcgammaRI. *Leukemia research*, *27*(8), 677–682. https://doi.org/10.1016/s0145-2126(02)00343-0

Komi, D., & Redegeld, F. A. (2020). Role of Mast Cells in Shaping the Tumor Microenvironment. *Clinical reviews in allergy & immunology*, *58*(3), 313–325. https://doi.org/10.1007/s12016-019-08753-w

Lyons, D. (2023). *REGULATORS OF MAST CELL ACTIVATION*. Scholarship & Creative Works @ Digital UNC. https://digscholarship.unco.edu/dissertations/960/

Majorini, M. T., Colombo, M. P., & Lecis, D. (2022). Few, but efficient: The role of mast cells in breast cancer and other solid tumors. *Cancer Research*. https://doi.org/10.1158/0008-5472.can-21-3424

Manore, S. G., Doheny, D. L., Wong, G. L., & Lo, H. W. (2022). IL-6/JAK/STAT3 Signaling in Breast Cancer Metastasis: Biology and Treatment. *Frontiers in oncology*, *12*, 866014. https://doi.org/10.3389/fonc.2022.866014

Min, H. K., Kim, K. W., Lee, S. H., & Kim, H. R. (2020). Roles of mast cells in rheumatoid arthritis. *The Korean journal of internal medicine*, *35*(1), 12–24. https://doi.org/10.3904/kjim.2019.271

Nagata, Y., & Suzuki, R. (2022). FcεRI: A Master Regulator of Mast Cell Functions. Cells, 11(4), 622. https://doi.org/10.3390/cells11040622

NAPHTHOL AS - D CHLOROACETATE METHOD FOR ESTERASE IN PARAFFIN SECTIONS AND SMEARS. Method of the histochemical stains and Diagnostic Application - Department of Pathology and Laboratory Medicine - University of Rochester Medical Center. (n.d.). Retrieved December 5, 2021, from https://www.urmc.rochester.edu/urmc-labs/pathology/stainsmanual/index.html

Okano, M., Oshi, M., Butash, A. L., Katsuta, E., Tachibana, K., Saito, K., Okayama, H., Peng, X., Yan, L., Kono, K., Ohtake, T., & Takabe, K. (2019, August 27). *Triple-negative breast cancer with high levels of annexin A1 expression is associated with mast cell infiltration, inflammation, and angiogenesis*. International journal of molecular sciences. Retrieved November 11, 2021, from https://www.ncbi.nlm.nih.gov/pmc/articles/PMC6747082/.

Protocol - Cell Surface Flow Cytometry Staining Protocol. (n.d.). https://www.biolegend.com/fr-ch/protocols/cell-surface-flow-cytometry-staining-protocol

Rasé, V. J., Hayward, R., Haughian, J. M., & Pullen, N. A. (2022). T_h17, T_h22, and Myeloid-Derived Suppressor Cell Population Dynamics and Response to IL-6 in 4T1 Mammary Carcinoma. *International journal of molecular sciences, 23*(18), 10299. https://doi.org/10.3390/ijms231810299

Ribatti, D., Tamma, R., & Crivellato, E. (2018). The dual role of mast cells in tumor fate. *Cancer Letters, 433*, 252-258. 10.1016/j.canlet.2018.07.005

Rubin, I., & Yarden, Y. (2001). *The Basic Biology of HER2*. Define me. Retrieved November 27, 2021, from https://www.annalsofoncology.org/article/S0923-7534(19)54455-6/pdf.

Russo. (2023). R2 Genomics Analysis and Visualization Platform [Dataset]. In *Defining the Genomic Signature of the Parous Breast*. https://hgserver1.amc.nl/cgi-bin/r2/main.cgi

Russo. (2023). R2 Genomics Analysis and Visualization Platform [Dataset]. In *Genomic signature of parity in the breast of premenopausal women*. https://hgserver1.amc.nl/cgi-bin/r2/main.cgi

Sinn. (2019). R2 Genomics Analysis and Visualization Platform [Dataset]. In *A robust 18-gene Predictor for Sensitivity to Endocrine Therapy for Metastatic Breast Cancer*. https://hgserver1.amc.nl/cgi-bin/r2/main.cgi

Travis, M. A., & Sheppard, D. (2014). TGF-β activation and function in immunity. *Annual review of immunology*, *32*, 51–82. https://doi.org/10.1146/annurev-immunol-032713-120257

Vita, A. A., & Pullen, N. A. (2022). Exploring the mechanism of berberine-mediated T_{fh} cell immunosuppression. *Phytomedicine: international journal of phytotherapy and phytopharmacology*, *105*, 154343. https://doi.org/10.1016/j.phymed.2022.154343